Monthly Notices
of the
ROYAL ASTRONOMICAL SOCIETY

MNRAS **480,** 4489–4504 (2018) doi:10.1093/mnras/sty2061

Optical observations of 'hot' novae returning to quiescence

P. Zemko,[1★] S. Ciroi,[1★] M. Orio,[2,3★] A. Odendaal,[4] S. Shugarov,[5,6] E. Barsukova,[7] A. Bianchini,[3] V. Cracco,[1] M Gabdeev,[7] V. Goranskij,[5] B. Tofflemire,[2] A. F. Valeev[7,8] and N. Katysheva[5]

[1]*Department of Physics and Astronomy, Università di Padova, vicolo dell'Osservatorio 3, I-35122 Padova, Italy*
[2]*Department of Astronomy, University of Wisconsin, 475 N. Charter Street, Madison, WI 53704, USA*
[3]*INAF - Osservatorio di Padova, vicolo dell' Osservatorio 5, I-35122 Padova, Italy*
[4]*Department of Physics, University of the Free State, 9300 Bloemfontein, South Africa*
[5]*Sternberg Astrophysical Institute, Lomonosov Moscow University, Universitetsky Ave., 13, Moscow 119992, Russia*
[6]*Astronomical Institute of the Slovak Academy of Sciences, Tatranská Lomnica, 059 60, The Slovak Republic*
[7]*Special Astrophysical Observatory, Russian Academy of Sciences, Nizhnij Arkhyz, Karachai-Cherkesia 369167, Russia*
[8]*Kazan Federal University, Kremlevskaya 18, 420008 Kazan, Russia*

Accepted 2018 July 25. Received 2018 July 23; in original form 2017 December 31

ABSTRACT

We have monitored the return to quiescence of novae previously observed in outburst as supersoft X-ray sources, using optical photometry of the intermediate polar (IP) V4743 Sgr and the candidate IP V2491 Cyg, and optical spectroscopy of these two and seven other systems. Our sample includes classical and recurrent novae, short-period (few hours), intermediate-period (1–2days) and long-period (symbiotic) binaries. The light-curves of V4743 Sgr and V2491 Cyg present clear periodic modulations. For V4743 Sgr, the modulation occurs with the beat of the rotational and orbital periods. If the period measured for V2491 Cyg is also the beat of these two periods, the orbital period should be almost 17 h. The recurrent nova T Pyx already shows fragmentation of the nebular shell less than 3 yr after outburst. While this nova still had strong [O III] at this post-outburst epoch, these lines had faded after 3 to 7 yr in all the others. We did not find any difference in the ratio of equivalent widths of high-ionization/excitation lines to that of the Hβ line in novae with short and long orbital periods, indicating that irradiation does not trigger a high mass-transfer rate $\dot{m}$ from secondaries with small orbital separation. An important difference between the spectra of RS Oph and V3890 Sgr and those of many symbiotic persistent supersoft sources is the absence of forbidden coronal lines. In combination with the X-ray turn-off, we interpret this as an indication that mass transfer in symbiotic recurrent novae is intermittent.

Key words: line: profiles – stars: novae, cataclysmic variables, HV Cet, V2491 Cyg, KT Eri, RS Oph, T Pyx, U Sco, V3890 Sgr, V4743 Sgr, V382 Vel, white dwarfs, binaries: symbiotic.

1 INTRODUCTION

Classical novae (CNe) are white dwarf (WD) binaries in which a large amount of accreted hydrogen-rich material results in a thermonuclear runaway from the surface of the WD. Although there is evidence that all novae have repeated outbursts, we define recurrent novae (RNe) as those with more than one nova explosion observed over human-life time-scales. Most RNe should host massive WDs accreting at a high rate (see, for instance, models by Wolf et al. 2013). In this paper, we present post-nova-explosion follow-ups of binaries with two types of secondaries: late-type main-sequence stars (cataclysmic variables) and red giants (symbiotic stars). The observations were carried out in the framework of a long-term project for monitoring novae that were well observed in outburst in the optical and X-ray as they returned to quiescence. Previous papers of this series include Zemko, Mukai & Orio (2015, hereafter Paper I) and Zemko et al. (2016, hereafter Paper II).

Novae are detected as bright sources in the optical band, but as the WD atmosphere contracts at rising temperature, the peak luminosity shifts towards shorter wavelengths. When the WD radius shrinks back to close to the pre-outburst size, the WD atmosphere, heated by the underlying hydrogen-burning, usually has a temperature high enough to peak in the supersoft X-ray range. If the ejected envelope

★ E-mail: polina.zemko@gmail.com (PZ); orio@astro.wisc.edu (SC); marina.orio@oapd.inaf.it (MO)

© 2018 The Author(s)
Published by Oxford University Press on behalf of the Royal Astronomical Society

Downloaded from https://academic.oup.com/mnras/article-abstract/480/4/4489/5078952
by Moscow State University, Scientific Library user
on 03 September 2018

is transparent to soft X-rays, the system is observed as a supersoft X-ray source (SSS) (e.g. Orio, Covington & Ögelman 2001a; Krautter 2008; Orio 2012). X-ray grating observations of novae in the SSS phase allow measurements of the chemical composition, the temperature of the WD atmosphere and the effective gravity. The latter two parameters give an estimate of the WD mass. The SSS phase can last from days to years and ends when the WD atmosphere cools (Orio 2012).

In Papers I and II we continued to observe two recent novae that appeared as luminous SSSs, namely V2491 Cyg (in the X-ray) and V4743 Sgr (in the X-ray and at optical wavelengths), and made two interesting discoveries: first, both novae show the diagnostics of intermediate polars (IPs), in which the accretion disc is disrupted by the moderately strong magnetic field of the WD (of the order of 10^6 G); second, in both cases the WD did not seem to cool isotropically, but the flux decreased by orders of magnitude, with the effective temperature apparently remaining high in a small region. We hypothesized that this region may reside at the poles and be caused by the magnetic nature of the WD. We show in this paper that the optical light curves of these two novae show further evidence of their IP nature.

Moreover, in this paper we analyse a collection of optical spectra taken after the end of the SSS phase of these and several other SSS-novae that have returned to quiescence. Several of the spectra we collected were taken in the spectral region in the wavelength range of the Hβ and the He II 4686-Å lines and the Bowen blend. The He II 4686-Å line requires an ionizing continuum source peaking in the range 200–300 Å; it is typical of binaries accreting at high $\dot{m}$, of recent novae and of IPs. The Bowen blend is 'pumped' by lines in the ultraviolet (UV) region. By studying the spectra of planetary nebulae, Bowen (1934, 1935) pointed out that, by a natural coincidence, a few UV resonance lines of He II, [O III] and N III have almost exactly the same wavelength. Bowen identified *excitation by secondary radiation*, or *line absorption by secondary quanta*: the decays of the above UV transitions produce the N III emission lines at optical wavelengths at 4640.64, 4641.85 and 4634.13 Å, and a subsequent decay causes two more transitions, N III at 4097.36 and 4103.39 Å. In addition, lines of [O III], C III and more rarely O II are also produced close to 4640–4650 Å, forming the so-called 'Bowen complex' or 'Bowen blend', which has now frequently been observed not only in planetary nebulae but also in X-ray binaries, symbiotic stars and novae. Additional decays, charge-exchange processes and a third 'Bowen cascade' in astronomical sources were analysed by Kastner & Bhatia (1996).

We also followed the development of the nebular, forbidden [O III] lines at 4959 and 5008 Å, in order to monitor the contribution of the nova shell to the optical emission.

In the next section we present a general overview of the objects studied in this paper. Section 3 describes the observations and data analysis; Section 4 focuses on our IP or IP-candidate novae; Section 5 describes the optical spectra of the short-period novae; Sections 6 focuses on two symbiotic novae; and Section 7 concludes the paper.

2 A BRIEF HISTORY OF OUR TARGETS

Table 1 lists the physical parameters known for each nova in our program. The first two objectsare the IP candidates, and are followed by the other novae in order of increasing orbital period. We have observed one recurrent nova below the period gap, two classical novae with periods of a few hours, two novae (recurrent and not) with periods of 1–2 d, two more suspected to have orbital periods in the same range, and finally two recurrent symbiotic novae.

2.1 V4743 Sgr

V4743 Sgr, a moderately fast nova, was discovered in outburst on 2002 September 20 by Haseda et al. (2002), when it was close to the 5th magnitude. V4743 Sgr continued nuclear burning for at least 1.5 yr after the outburst (Rauch et al. 2010). A modulation of the X-ray light-curve on a time-scale of 22 min, reported by several authors (see Paper II and Ness et al. 2003; Leibowitz et al. 2006; Dobrotka & Ness 2010), revealed that this binary system hosts a magnetic WD. The orbital period (∼6.7 h) and a proposed beat period between the orbital and the spin period (∼24 min) were detected in the optical band by Kang et al. (2006), Richards et al. (2005) and Wagner et al. (2005).

The distance to the nova is uncertain. The estimates range from 1.2 kpc (Nielbock & Schmidtobreick 2003) to 3.9 kpc (Vanlandingham et al. 2007). Nielbock & Schmidtobreick (2003) found that the distance cannot exceed 6 kpc.

2.2 V2491 Cyg

V2491 Cyg (Nova Cyg 2008b) was discovered by Hiroshi Kaneda on 2008 April 10.728 at V=7.7 (Nakano et al. 2008). The nova was very fast and its light-curve showed an unusual feature – a short 're-brightening' at the end of April. Jurdana-Sepic & Munari (2008) discovered the optical counterpart of the nova at pre-outburst magnitude $V\simeq$17.1, with a short dimming before the outburst. Although no previous outburst was detected, V2491 Cyg shares many properties with RNe (see the discussion in Paper I). Pre-outburst X-ray observations of V2491 Cyg revealed that the WD was accreting at a high rate (Ibarra et al. 2009), and the high WD atmospheric temperature measured during the SSS phase indicates that the WD is also very massive (Ness et al. 2011). There are also several indications that the WD in V2491 Cyg is magnetic (see Paper I, and Hachisu & Kato 2009; Ibarra et al. 2009; Takei et al. 2011). The best (albeit indirect) proof of an IP is a modulation of the soft X-rays with the rotation period of the WD. This period may be the ∼38-min one measured both in the optical and in the X-ray, but it was unclear whether it was stable (in addition to Paper I, see Shugarov et al. 2010; Darnley et al. 2011; Ness et al. 2011). However, in more recent, still unpublished,

XMM–Newton data this period has been detected again with higher confidence and it does indeed seem to be stable. Thus, it is very likely to be the rotation period of the WD (Orio et al. 2018, in preparation). The orbital period of the system is not known. Baklanov, Pavlenko & Berezina (2008) detected a modulation with a period of 0.09580(5) d between 10 and 20 d after the outburst, but this has not been measured again in more recent works (Shugarov et al. 2010; Page et al. 2010; Darnley et al. 2011).

2.3 T Pyx

T Pyx is a RN that had outbursts in 1890, 1902, 1920, 1944, 1967 and 2011 (see Gilmozzi & Selvelli 2007; Selvelli et al. 2008; Schaefer 2010; Schaefer et al. 2013, for a review). The explosions are typically slow, with t_2=32 and t_3=62 d, respectively (Schaefer 2010). The outburst light-curves show day-to-day oscillations of 0.5–1.0 mag. Patterson et al. (1998) have shown that, apart from a dominant stable periodicity of 0.0762264(4) d, which has been attributed to orbital variation, there are weaker signals at 0.1098 and 1.24

Downloaded from https://academic.oup.com/mnras/article-abstract/480/4/4489/5078952
by Moscow State University, Scientific Library user
on 03 September 2018

Table 1. Properties of the novae.

Object	Outburst maximum	Ampl. [V mag]	t_2 [d]	t_3 [d]	P_{orb} [d]	M_{WD} [$M_\odot$]	Distance [kpc]	$E(B\text{-}V)$ [mag]	Class
V4743 Sgr	2002/09/20[h1]	$\gtrsim$11.2	6[s]	12[s]	0.28[h2]	1.1-1.2[h3]	$3.90^{+2.37}_{-1.19}$	0.12[h4]	CN
V2491 Cyg	2008/04/11[c1]	$\gtrsim$9	4[s]	16[s]		1.3[c2]	$4.53^{+4.81}_{-2.63}$	0.43[c3]	CN (RN?)
T Pyx	2011/05/11[e0]	9.1[e1]	32[e1]	62[e1]	0.076[e2]	1.25-1.4[e3]	$2.93^{+0.41}_{-0.33}$	0.35[e2]	RN
V382 Vel	1999/05/23[d1, d2]	14. 3	6[s]	13[s]	0.1461[d3]	1.1-1.2[d2]	$1.71^{+0.18}_{-0.15}$	0.2[d5]	CN
KT Eri	2009/11/14[b1]	$\sim$9	$\sim$6[b1, b2]	14.7[b2]			$3.69^{+0.53}_{-0.42}$	0.08[b3]	CN (RN?)
U Sco	2010/01/28	10.1[e]	1.2[e]	2.6[e]	1.23[g1]	$>$1.37[g2, g3]	$6.56^{+3.57}_{-1.35}$	0.24[g4]	RN
HV Cet	$\leq$2008/07/17	$>$6			$\sim$1.7[a1, a2]		$\sim$2.5[a1, a3]	0.146[a4]	CN
RS Oph	2006/02/13[f1]	6.2[e]	6.8[e]	14[e]	453.6[f2]	$\geq$1.2[f4]	$2.14^{+0.28}_{-0.22}$, 1.4[f3]		RN, Symb.
V3890 Sgr	1990/04/27	7.4[e]	6.4[e]	14.4[e]	519.7[e]		$4.36^{+2.36}_{-1.32}$		RN, Symb

Notes: Except for HV Cet, distances have been obtained from the GAIA data base using ARI's Gaia Services at http://gaia.ari.uni-heidelberg.de/tap.html. We also give a pre-GAIA alternative estimate for RS Oph, because the symbiotic's nebula and disc can make the parallax determination more uncertain than the nominal uncertainty in the data base. The other references are as follows: [a1]Beardmore et al. (2012), [a2]Goranskij & Metlova (2009), [a3]Schwarz et al. (2008), [a4]Schwarz et al. (2011), [b1]Hounsell et al. (2010b), [b2]Imamura & Tanabe (2012), [b3]Ragan et al. (2009), [c1]Munari et al. (2011), [c2](Hachisu & Kato 2009), [c3]Rudy et al. (2008), [d1]Gilmore & Kilmartin (1999), [d2]Della Valle et al. (2002), [d3]Bos et al. (2001), [d4]Shore et al. (2003), [d5]Cardelli, Clayton & Mathis (1989) and Augusto & Diaz (2003) for discussion, [e0]see for a review Schaefer et al. (2013), [e1]from fig. 4 of Surina et al. (2014), [e2]Patterson et al. (1998), [f1]Hounsell et al. (2010a), [f2]Brandi et al. (2009), [f3]Barry et al. (2008), [f4]Nelson2008, [g1]Schaefer (1990), [g2]Thoroughgood et al. (2001), [g3]Hachisu et al. (2000), [g4]Burstein & Heiles (1982), [h1]Haseda et al. (2002), [h2]Kang et al. (2006); Richards et al. (2005); Wagner et al. (2005), [h3]Nielbock & Schmidtobreick (2003), [h4]Zemko et al. (2016), [s]Strope, Schaefer & Henden (2010).

d. The orbital period increases on a time-scale $P/\dot{P} = 3 \times 10^5$ yr (Patterson et al. 2014), and from the orbital period change Patterson et al. (2014) inferred that, although the WD in T Pyx is very massive ($\sim$1.35 $M_\odot$ Selvelli et al. 2008), the ejected mass exceeds the amount of accreted material. The same result was found by Selvelli et al. (2008) by modelling *IUE* observations. The X-ray spectra show that the central source never became completely visible, probably because of obscuration by the ejecta (Tofflemire et al. 2013).

2.4 V382 Vel

The outburst of V382 Vel was discovered independently by P. Williams and A. C. Gilmore on 1999 May 22 (Williams et al. 1999). It was one of the brightest nova ever observed, with $V_{max} \sim 2.3 \pm 0.1$ (Della Valle et al. 2002). V382 Vel was classified as a fast oxygen-neon nova (Woodward et al. 1999). Oxygen-neon (hereafter, ONe) novae are rich in these two elements, that are thought to be dredged up from an underlying ONe WD. The high optical luminosity at maximum and the short turn-off time of the super-soft X-rays (Ness et al. 2005) implies that the nova hosts a massive WD, probably in the mass range 1.1–1.2 $M_\odot$ (Della Valle et al. 2002). Della Valle et al. (2002) estimated the distance to be 1.70 $\pm$ 0.34 kpc, while Shore et al. (2003) found a value of 2.5 kpc. Bos et al. (2001) reported that the orbital period of the binary is 0.14615(1) d, which was later confirmed by Balman, Retter & Bos (2006).

2.5 KT Eri

KT Eri was discovered by K. Itagaki on 2009 November 25.536 UT (Itagaki 2009) at 8.1 mag after maximum-light. From the Catalina Sky Survey (CSS) data, Drake et al. (2009c) found that the outburst occurred between 2009 November 10.41 UT and 18 UT, and Hounsell et al. (2010b) constrained the time of the outburst to 2009 November 14.67 $\pm$ 0.04 UT using the USAF/NASA Solar Mass Ejection Imager (SMEI) onboard the *Coriolis* satellite. The nova was very fast: t_2 and t_3 were $\sim$6 d (Hounsell et al. 2010b; Imamura & Tanabe 2012) and 14.7 d (Imamura & Tanabe 2012), respectively. Jurdana-Šepić et al. (2012) studied historical light-curves of KT Eri and found that the progenitor system had $\langle B \rangle = 14.7 \pm 0.4$ and probably contained an evolved secondary. Although several properties of KT Eri make it similar to RNe, no previous outburst was detected (for a review see Jurdana-Šepić et al. 2012). The authors also found two periodicities, of 737 and 367 d. From the Swift archive, we found that KT Eri was a very luminous SSS until about 300 d after the outburst (see also Ness et al. 2014).

2.6 U Sco

U Sco is a well-studied RN (for a review see Schaefer 2010; González-Riestra 2015). A total of 10 outbursts of U Sco have been detected: in 1863 and then every 10 $\pm$ 2 yr, with the last one on 2010 January 28 (Schaefer et al. 2010). The orbital period of the system is 1.2344 d (Schaefer 1990). Nova eruptions in U Sco occur on very short time-scales: the rise to maximum is 6–12 h, t_2 and t_3 are 1.2 and 2.6 d, respectively, and the return to quiescence is 67 d (Schaefer 2010; Pagnotta et al. 2015). U Sco hosts a very massive WD ($>$1.37 $M_\odot$ Hachisu et al. 2000; Thoroughgood et al. 2001), and the ejecta velocity reaches 10 000 km s^{-1} (González-Riestra 2015). At maximum it is usually around V=7.5 mag, in quiescence $\sim$ 17.5 mag, and during the total eclipse 18.9 mag (Schaefer 2010). The short SSS phase was observed in the last outburst only through Thomson-scattering reflected emission, because the system has high inclination, and it has been described by Ness et al. (2012) and by Orio et al. (2013).

2.7 HV Cet

CSS081007:030559+054715 (HV Cet) was discovered by the Catalina Real-time Transient Survey (CRTS) on 2008 October 7 (Drake et al. 2009b). Observed as it was coming out of the Sun, it brightened by about 4 mag in less than 1 yr and was classified as a possible RN of the ONe class; however, the time of the maximum was unknown (Pejcha, Prieto & Denney 2008). We collected pho-

Downloaded from https://academic.oup.com/mnras/article-abstract/480/4/4489/5078952
by Moscow State University, Scientific Library user
on 03 September 2018

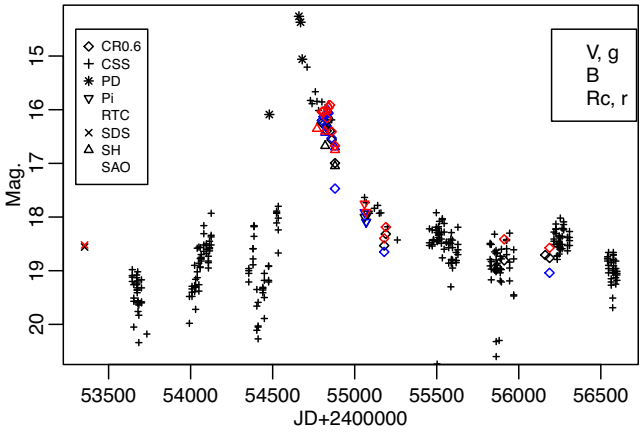

Figure 1. The long-term light curves of HV Cet in the *B* (blue), *V, g* (black) and *Rc, r* (red) filters, covering the nova outburst. Because the nova was intensively monitored during the decline, in the interval between JD 2454600 and JD 2455300 we have plotted the 10-d averaged magnitudes. CR0.6, Goranskij & Metlova (2009); CSS, the Catalina Sky Survey (CSS) data (Drake et al. 2009a); PD, Prieto et al. (2008); SDS and RTC, *g*, *r* magnitudes from SDSS and RETROCAM from Prieto et al. (2008); SAO and Pi, *BVRc* photometry performed by V. Goranskij with the 1-m Zeiss telescope of the Special Astrophysical Observatory of the Russian Academy of Sciences (SAO RAS) and with the Sternberg Astronomical Institute (SAI) Crimean Station 0.5-m Maksutov meniscus telescope (AZT-5); SH, *BVRc* photometry performed by S. Shugarov with the 0.5-m telescope G1 of the Stara Lesna Observatory, Slovakia.

tometric observations from several surveys and observers in order to bridge the observational gap as much as possible and we present a previously unpublished outburst light-curve of HV Cet in Fig. 1, which includes still unpublished photometric measurements. Unfortunately, however, the nova was behind the Sun during the peak and the initial decline, possibly even while it declined by several magnitudes. There is evidence that it may have been a fast nova, because of the high ejecta velocity.

Several possible periodic variations in the X-ray, UV and optical were reported during the late outburst phase in which the nova was monitored. Beardmore et al. (2012) investigated the X-ray, UV and optical evolution, including the American Association of Variable Star Observers (AAVSO) light-curve and GALEX observations, and reported a modulation with a period of 1.77 d. Goranskij & Metlova (2009) monitored the nova at quiescence in the *B*, *V* and *Rc* filters and measured two periods: 1.694(5) and 0.6106(6) d, which surprisingly were not detected in pre-outburst light-curves (Drake et al. 2009b). Drake et al. (2009b) also measured the optical polarization, and no significant circular polarization was found.

2.8 RS Oph

RS Ophiuchi is a symbiotic RN that undergoes thermonuclear runaways every 9 to 21 yr. Six outbursts have been detected (in 1898, 1907, 1933, 1958, 1967, 1985 and 2006) and another two, in 1907 and 1945, were missed owing to a seasonal gap but were later partially detected by Schaefer (2010) and Adamakis et al. (2011). RS Oph hosts a M0–2 III giant component of mass 0.68–0.80 $M_{\odot}$ (Brandi et al. 2009), and the short recurrence time of the outbursts implies a massive WD with a mass of at least 1.2 $M_{\odot}$ (Mikołajewska & Shara 2017; Brandi et al. 2009). The orbital period of the system is 453.6 d (Brandi et al. 2009). The high mass-transfer rate (Booth, Mohamed & Podsiadlowski 2016) and evidence of a massive WD make it a good candidate Type Ia SN progenitor. During the most recent outburst, RS Oph was intensively observed from the radio to the X-ray. The X-ray evolution from a hard source originating in the shocked circumstellar material to an SSS has been described by Ness et al. (2007), Nelson et al. (2008) and Ness et al. (2009). It was imaged with the *Hubble Space Telescope* (Ribeiro et al. 2009), and observed in the infrared by Chesneau et al. (2007). Radio interferometry (O'Brien et al. 2006) revealed bipolar outflows interacting with dense circumstellar material (see e.g. Bode et al. 2006; Sokoloski, Rupen & Mioduszewski 2008; Eyres et al. 2009; Vaytet et al. 2011, and references therein). Iijima (2009) followed the spectral evolution of RS Oph after the 2006 outburst and found a short-lived flare-up of He I emission lines, which they attributed to a helium flash (we note in passing, however, that this interpretation is debatable). Many emission lines in the post-outburst spectra had a central narrow component, blue- and red-shifted wings, and a very broad component (Iijima 2009).

The quiescence optical spectra of RS Oph are characterized by a complex structure of Balmer emission lines and a pronounced variability on various time-scales. The Hα emission line has a narrow component (the full width at half-maximum, or FWHM, is $\sim$220 km s^{-1}), a highly variable broad component (FWHM$>$2000 km s^{-1}), and a narrow absorption component (Zamanov 2011), slightly blue-shifted with respect to the narrow one, which disappears during the outbursts (Brandi et al. 2009). This absorption component does not follow the motion of the stellar components of the binary system (Brandi et al. 2009). The Hα line also has a very broad base, with full width at zero intensity, or FWZI, $\approx$4600 km s^{-1} (Zamanov 2011). Worters & Rushton (2014) performed high-time-resolution spectroscopy of RS Oph and found that the equivalent width (EW) of the double-peaked Hα is variable on a time-scale as short as 2 min, while the ratio of the blue to red peak remains approximately constant. These authors did not find a correlation between the variability of the Hα line and the strength of other lines, proposing that the variation is intrinsic to Hα and is probably related to changes in the photoionization of the nebula. In order to explain the variability of the broad component of Hα, Zamanov (2011) proposed several mechanisms, including blobs of matter, variable disc winds and an asymmetric Keplerian disc. Pavlenko et al. (2016) also proposed accretion disc variability as an explanation of the variation of the spectral energy distribution and intensity of the emission lines on time-scales of $\simeq$1 d. Even if it is not clear whether the secondary does fills its Roche lobe, RS Oph almost certainly hosts an accretion disc, probably as do many other symbiotics (see references and the discussion in Orio et al. 2017).

2.9 V3890 Sgr

The symbiotic RN V3890 Sgr was discovered as a CN in 1962 (Duerbeck 1987), and on 1990 April 27 it underwent a second outburst (Kilmartin et al. 1990). Although it did not initially belong to our program because it was observed optically only sparsely and there is only one serendipitous X-ray observation at a late outburst phase (Orio, Covington & Ögelman 2001b), we obtained a low-resolution spectrum that we include for comparison with RS Oph.

3 OBSERVATIONS AND DATA ANALYSIS

3.1 Photometry

We proposed Kepler observations of V4743 Sgr in the framework of the K2 campaign (field no. 7). The details of the observations are

Downloaded from https://academic.oup.com/mnras/article-abstract/480/4/4489/5078952
by Moscow State University, Scientific Library user
on 03 September 2018

Table 2. Summary of observations.

Object	Date of obs.	ΔT[a] [yr]	Exposure time [s]	Instrument[b]
		Photometry		
V4743 Sgr	2015/10/04–2015/12/26	13.1	18000	Kepler
V2491 Cyg	2015/06/16–18	7.2	120-180	WIYN 0.9m, *UBVRI*
	2015/07/17–23	7.3	90-300	SAI-Crimea 1.25m, *C*
		Spectroscopy		
V2491 Cyg	2008/06/08 23:59:10–00:53:04	0.2	600,1200,2400	Zeiss 1000 UAGS 325/4
	2009/07/30 22:38:55–23:05:31	1.3	420,440,600	BTA SCORPIO VPHG1200G
	2012/08/17 00:03:40–00:20:13	4.4	2 × 900	BTA SCORPIO VPHG550G
	2015/08/23 18:31:25–20:17:16	7.4	16 × 300	BTA SCORPIO VPHG1200B
T Pyx	2012/12/06 23:40:57	1.6	620	SALT RSS PC00000 PG2300
	2014/03/01	2.8	480	SALT HRS R=14,000
V382 Vel	2012/07/10 17:15:40	13.1	1700	SALT RSS PC00000 PG2300
	2013/04/30 21:08:38–21:58:57	13.9	4 × 990	SALT RSS PC00000 PG2300
KT Eri	2010/01/22 17:51:47-18:52:46	0.2	4 × 1200	Zeiss-1000 UAGS 325/4
	2010/12/06 21:05:53-21:09:56	1	150,462	BTA SCORPIO VPHG1200G
	2011/12/23 20:13:59	2	695	BTA SCORPIO VPHG550G
	2012/10/19 00:31:50-00:39:25	3	2 × 400	BTA SCORPIO VPHG550G
	2012/11/22 20:52:48	3	1000.2	SALT RSS PC00000 PG2300
U Sco	2013/05/01 02:37:52–02:58:03	3.2	2 × 1194	SALT RSS PC00000 PG2300 PL0150N001
	2013/05/01 21:43:02–22:01:39	3.2	2 × 1100	SALT RSS PC03850 PG0900
	2013/05/28 00:45:19–01:03:58	3.3	2 × 1100	SALT RSS PC03850 PG0900
	2013/06/10 23:54:14–00:12:53	3.4	2 × 1100	SALT RSS PC03850 PG0900
HV Cet	2013/11/05	3.3	2 × 1060	SALT RSS PC00000
RS Oph	2011/09/15 18:18:31–19:27:44	5.6	600,1200,1800	SAAO grating 4
	2011/09/16 19:57:16–21:27:48	5.6	4 × 1200	SAAO grating 4
	2011/09/19 19:48:33–20:52:49	5.6	2 × 600,2 × 1200	SAAO grating 5
	2011/09/20 20:07:59–20:52:11	5.6	4 × 600	SAAO grating 5
	2012/09/14 19:03:45–19:45:44	6.6	2 × 1200	SAAO grating 4
	2012/09/16 18:39:09–19:23:03	6.6	1200,2 × 600	SAAO grating 5
V3890 Sgr	2011/09/16 18:14:56–19:43:29	21.4	1200,2 × 1800	SAAO grating 4
	2011/09/17 18:33:16–20:40:50	21.4	6 × 1200	SAAO grating 5
	2011/09/19 18:14:35–19:38:19	21.4	4 × 1200	SAAO grating 5
	2011/09/20 18:00:58–19:33:30	21.4	4 × 1200	SAAO grating 5
	2012/09/15 20:18:08–21:20:32	22.4	2 × 1800	SAAO grating 4
	2012/09/18 20:21:46–21:48:19	22.4	3 × 1800	SAAO grating 5

Notes: [a]Time since the outburst maximum, [b]RSS, Robert Stobie Spectrograph; HRS, High-Resolution Spectrograph; PC00000, clear filter; PC03200, PC03400, PC03850, UV blocking filters; PC04600, blue blocking filter.
Grating wavelength ranges: PG0900, 3200–7100 Å; PG2300, 4200–5600 Å; VPHG1200G, 4000–5800 Å; VPHG550G, 3700–7800 Å; VPHG1200B, 3700–5500 Å; SAAO grating 4, 4000–4900 Å; SAAO grating 5, 6200–7000 Å.

given in Table 2. Both short-cadence (2-min) and long-cadence (30-min) light-curves were obtained. The analysis of the short-cadence light-curve is currently in progress, and we discuss here only the long-cadence light-curve.

Photometric observations of V2491 Cyg were performed with the 0.9-m WIYN telescope of the Kitt Peak National Observatory (KPNO) and the 1.25-m telescope of the Crimean Station of the Sternberg Astronomical Institute of Moscow University. During the KPNO observations, we measured the mean magnitudes of V2491 Cyg in the *U*, *B*, *V*, *R* and *I* filters and monitored the nova in the *V* filter. For better accuracy, the SAI Crimean Startion observations were performed without a filter. For absolute magnitude calibration we used the 112 822 star from the Landolt Equatorial Standards catalog (Landolt 1992). The mean absolute magnitudes and the errors are in Table 3.

3.2 The spectra

Spectroscopic observations were performed with the 10-m Southern African Large Telescope (SALT), with the Cassegrain spectrograph on the 1.9-m telescope of the South African Astronomical Observatory (SAAO),[1] with the 6-m Big Azimuthal Telescope (BTA) and with the 1-m Zeiss telescope of the Special Astronomical Observatory of the Russian Academy of Sciences (SAO RAS). The observations performed with the SAAO 1.9-m telescope will simply be referred to throughout the paper as the SAAO observations. The observation dates, exposure times and specific instruments used are summarized in Table 2.

[1]http://www.saao.ac.za/wp-content/uploads/sites/5/spmanv6.5.pdf

Downloaded from https://academic.oup.com/mnras/article-abstract/480/4/4489/5078952
by Moscow State University, Scientific Library user
on 03 September 2018

Table 3. *U*, *B*, *V*, *R* and *I* magnitudes of V2491 Cyg.

Filter	*U*	*B*	*V*	*R*	*I*
Mag.	18.27 ± 0.07	18.72 ± 0.08	18.03 ± 0.03	17.72 ± 0.03	17.41 ± 0.02

Two SALT instruments were used: the High-Resolution Spectrograph (HRS) and the Robert Stobie Spectrograph (RSS). The HRS was used in its low-resolution mode (resolving power $R = 14\,000$). All the SALT observations were performed in long-slit mode; some of them were obtained with the PG2300 grating to cover the 4200–5600 Å range, where our main lines of interest are, while others were taken with the PG900 grating to cover the 4200–7100 Å range, including the prominent Hα line. The width of the slit was 1 arcsec in both the SALT and the BTA observations, and 1.51 arcsec in the SAAO ones. The SALT and the BTA spectra were flux-calibrated with spectrophotometric standard stars, although SALT is a telescope with a variable pupil, which makes absolute flux calibration impossible. For the SALT spectra, therefore, we give only relative fluxes. All the flux-calibrated spectra were also dereddened with the values of $E(B-V)$ given in Table 1. The 1.9-m SAAO spectra were not flux-calibrated because spectrophotometric standards were not observed on those nights. Nevertheless, by making use of relative counts, we were able to compare the EWs of the lines and the flux ratio of lines next to each other. The emission-line fluxes and EWs were calculated by fitting Gaussian components (when the shape of a line was complex, we used several Gaussians). For the Bowen blend, we followed McClintock, Canizares & Tarter (1975), as illustrated in Fig. 5, using the same main component lines, including several lines of O II at about 4687 Å, that these authors introduced for X-ray binaries in which gaseous matter is irradiated by X-rays (at higher temperatures than the SSS in novae, at almost 10 $R_\odot$ distance).

In order to calculate the errors of the flux and EW of each line we repeated the following procedure 1000 times: we introduced a normally distributed noise with the same standard deviation as in the continuum to the Gaussian line profile and repeated the Gaussian fitting. The values we give for the flux and EW are the mean of the set of these 1000 measurements, and the errors were found from its standard deviation.

4 EXPLORING THE MAGNETIC NATURE OF V4743 SGR AND V2491 CYG

4.1 V4743 Sgr

The 30-min-cadence light-curve of V4743 Sgr was extracted using the K2SFF tool (Vanderburg & Johnson 2014).[2] The top-left panel of Fig. 2 shows this light-curve, which is highly variable on a time-scale of several days, with an amplitude exceeding 2 mag, but without a definite periodicity. We divided the light-curve into 1-d segments and removed the long-term variations with a third-order polynomial fitting for each segment. The de-trended light curve is presented in the top-right panel of Fig. 2. We then applied the Lomb–Scargle algorithm (Scargle 1982) to search for periodic modulations. The middle panels show spikes in the Lomb-Scargle periodograms (LSP), which correspond to the orbital period (6.684 h) and to the beat period between the orbital and the spin periods (23.65 min). Taking into account these two periodicities and the period found in the X-ray light-curves (Paper II and Dobrotka & Ness 2010), the relationship $1/P_{spin} - 1/P_{orb} = 1/P_{beat}$ is perfectly satisfied, thus confirming the result of Kang et al. (2006), who measured the beat of the orbital and WD rotation periods. This implies that the WD spin period is stable and provides even stronger evidence for our classification of V4743 Sgr as an IP in Paper II.

4.2 V2491 Cyg

Our X-ray observations of V2491 Cyg (Paper I) revealed that it is likely to be an IP (see Section 2.2). As shown in Fig. 3, we combined the KPNO and SAI-Crimean photometric observations, removed possible long-term variations from each nightly light-curve using polynomial fitting of order 1–4 (the order of the polynomial function was chosen according to the length of observation during each night), and performed a timing analysis with the Lomb–Scargle algorithm. We also analysed the combined data set with the Deeming (1975) method of descrete Fourier transform for arbitrarily distributed time series. In this analysis, the long-term variations were decomposed into several harmonic components, which were removed from the series using a pre-whitening procedure. The peaks around two frequencies, 0.0276 and 0.032 d respectively, appear independently in the method we apply. We found that the frequencies close to the one with the highest probability in each group are daily aliases. We did not find any reliable modulation on longer time-scales, because for periods longer than 0.045 d different methods yield slightly different results, and we concluded that, with the nature and quality of the data at hand, we cannot detect such frequencies with confidence. The data do not allow us to investigate the peaks around 0.032 d either. These peaks comprise four different frequencies that are most probably different sinusoidal components of a weak, quasi-periodic signal.

The highest peak is the one at 0.0276 d (36.24 min), and although the signal is low, this finding may be very important in the context of the magnetic interpretation of V2491 Cyg presented in Paper I. In fact, this period is only slightly shorter than the one of 0.0266 d (38 min) detected in the X-ray, and thus a possible interpretation is that it is the beat of the rotational and orbital period, as a result of the reprocession of the X-rays from the surface of the secondary on to the magnetic WD. If this interpretation is correct, taking our measurements of the putative spin and beat periods into account the orbital period should be about 0.7 d (16.8 h), which is too long to be detectable in our observations.

The optical spectra of V2491 Cyg are presented in Figures 4–6. All the spectra were flux-calibrated and dereddened. Fig. 4 shows the evolution of the optical spectrum from the outburst to quiescence. Because the outburst spectra of V2491 Cyg were studied in detail by Ribeiro et al. (2011), we focus here on the spectra obtained for one year after the explosion. We note here only that we confirm that the emission lines in outburst have a complex saddle-like structure with wings, extending up to 4600 km s^{-1}, and, considering the discussion of Ribeiro et al. (2011), our outburst spectrum is consistent with their model A (polar blobs with an equatorial ring) but it has a stronger contribution from the component associated with the equatorial ring.

The [O III] line, originating in the nova shell, was weak but still visible in the spectra obtained 4.3 and 7.3 yr after the outburst. The main features of the quiescent spectra are the Balmer lines, the He II λ4686 line and the Bowen blend λλ4640–4650. All the emission lines in the quiescent spectra are single-peaked (except for the [O III] line, originating in the nova shell), which is probably the result of a low orbital inclination.

[2] https://archive.stsci.edu/k2/hlsp/k2sff/search.php

Downloaded from https://academic.oup.com/mnras/article-abstract/480/4/4489/5078952
by Moscow State University, Scientific Library user
on 03 September 2018

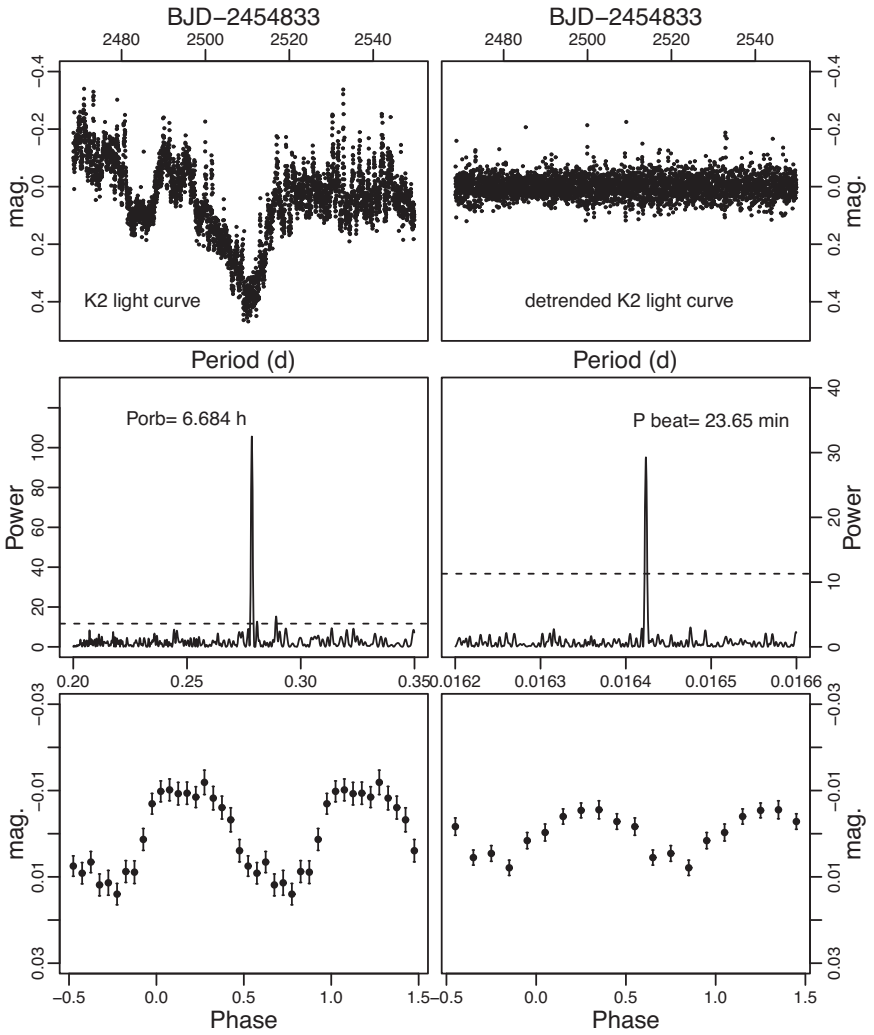

Figure 2. (Top) the original (left) and de-trended Kepler light curves of V4743 Sgr. (Middle) LSP of the detrended Kepler light curve showing the orbital (left) and the beat (right) period. The horizontal dashed line shows the 0.3 per cent false alarm probability. (Bottom) the light-curve folded with the orbital (left) and the beat (right) periods.

The fact that the orbital period has never been detected in this system, either photometrically or spectroscopically, may imply that the inclination is lower than $\sim 60^{\circ}$. Limits on the inclination can also be derived from the lack of a double-peaked profile. The resolution of the optical spectra, presented in this work, was 5.6 Å in 2009, 15.8 Å in 2012, and 6 Å in 2015. Such resolution would allow the measurement of line separations of 190–360 km s^{-1}; however, we did not detect any line-splitting because of the Keplerian motion in the accretion disc. If V2491 Cyg is an IP with $M_{\rm WD}$=1.2 M$_{\odot}$, the Keplerian velocity at the synchronization radius corresponding to the proposed 38-min rotation period is 760 km s^{-1}. In the case of non-magnetic accretion, the maximum plasma velocity in the accretion disc is even higher. If the Balmer lines in the V2491 Cyg spectra originate from the accretion disc, the absence of the double-peaked profiles gives an upper limit for the inclination of $\arcsin(190/760) = 14^{\circ}$.

In order to analyse the evolution and the shape of the emission lines of V2491 Cyg, we localized the regions of the HeII λ4686 and the Balmer lines and attempted to fit them with a number of Gaussians after removing the continuum using the `'continuum'` task in IRAF. The result of the fit is marked with the red solid line, and the Gaussian components are marked with the black dashed lines in Figs 5 and 6.

An interesting fact that we want to emphasize is that almost all the Balmer lines and the HeII λ4686 line in the 2012 and 2015 spectra have two components, red- and blue-shifted, with the same velocity of ∼760 km s^{-1} (see Figs 5 and 6). Double or multiple components in the emission lines are quite typical of IPs (see for instance Ferrario 1991), and in fact we notice that this spectrum resembles that of GK Per, a well-known IP, where similar emission-line components were detected during the dwarf nova outburst and were interpreted as emission from the accretion curtain near the magnetized WD (Morales-Rueda, Still & Roche 1999; Bianchini et al. 2003). Although some of these line components in V2491 Cyg are weak and are comparable with the noise level, the same velocities and their presence in two spectra, obtained 3 yr apart, indicate that they must be real. This analogy with GK Per further supports the IP model for this nova. It can be argued that, if the nova shell were larger than the slit width, we could lose light with zero radial velocity and detect only the light from the material moving from and towards the observer. The slit width was 1 arcsec, and assuming the same expansion velocity as measured during the

Downloaded from https://academic.oup.com/mnras/article-abstract/480/4/4489/5078952
by Moscow State University, Scientific Library user
on 03 September 2018

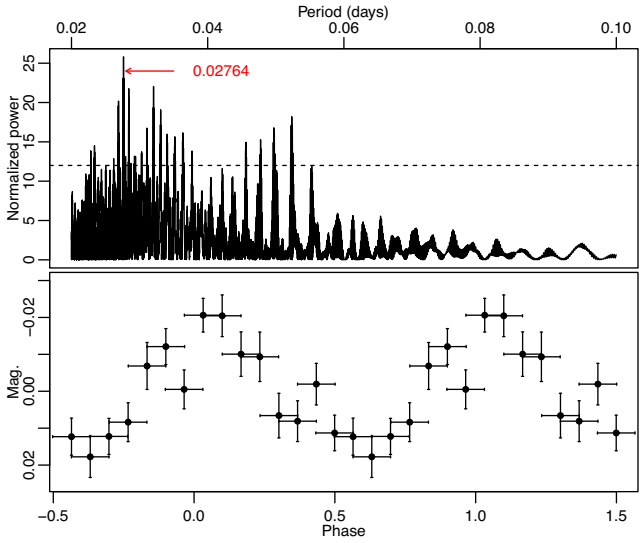

Figure 3. (Top) LSP of the KPNO and SAI Crimean Station observations of V2491 Cyg. The highest peak, marked with the red arrow, corresponds to the 0.02764-d period. The horizontal dashed line represents the 0.3 per cent false alarm probability. (Bottom) the light-curve folded with the 0.02764-d period.

outburst, 4600 km s^{-1}, and a distance of 10 kpc, the upper limit for the shell angular dimension is only 0.38 arcsec, so we can exclude this possibility. The line components can also be the effect of visibility of the accretion disc at different orbital phases, but because our exposures were probably shorter than the orbital period, as we did not detect any reliable modulation with periods in the range 0.05–0.2 d, this explanation cannot be accepted.

Another possible explanation for the two components in the emission lines, other than the IP nature, is the presence of a wind from the binary system; however, in this case we would expect a broad line component, rather than two narrow components with the same velocity. A third possibility, which we cannot rule out at this stage, is that the two components are caused by a bipolar outflow.

5 THE SPECTRA OF THE NON-SYMBIOTIC NOVAE

5.1 T Pyx

Fig. 7 shows the spectrum of T Pyx obtained on 2014 March 3 with the SALT high-resolution spectrograph (HRS). It is compared with the RSS spectrum obtained on 2012 December 12 by Tofflemire et al. (2013), in the region 4900–5050 Å (top panel). We show also a proposed multicomponent fit for the strongest lines, He II λ4686 and Hβ in the middle panel, and [OIII] in the bottom panel. In this nova, the nebular lines of [O III] appear to be much stronger than in other novae observed at comparable post-outburst epochs, as the spectra of other novae shown in this paper indicate. The insets zoom into the Hβ and HeII lines. All the lines have a complicated structure, with a broad component at zero velocity and some narrow components shifted by ± 200–1200km s^{-1}.

Because we cannot measure absolute fluxes with SALT, we are comparing here the flux-normalized spectra, focusing on the emission lines. We see that both He II λ4686 and Hβ appear to have become more prominent, and we still see a saddled profile that originates in an accretion disc. Three years after the outburst, unlike in most other novae, the [OIII] lines are still prominent and show a very complex profile with multiple components. This result indicates that the fragmentation of the shell that produces the clumps and knots observed in the shell of the previous outbursts (Shara et al. 1997) occurs at an early stage, seemingly contradicting the model of Toraskar et al. (2013) in which a Richtmyer–Meshkov instability (the equivalent of a Raleigh–Taylor instability in an accelerated gas) occurs long after the outburst, causing fragmentation.

5.2 The evolution of the spectrum of KT Eri

The evolving spectrum of KT Eri from outburst to quiescence is presented in Fig. 8. In this figure we show the normalized spectra, for reasons of clarity. The spectrum obtained 1 yr after the outburst shows prominent inverse P Cyg profiles of the Balmer lines. None of the spectra obtained at other epochs show similar profiles. These absorptions also show a prominent gradient: the absorption feature of the Hβ line is stronger than that of the Hγ line. We checked that these absorptions are not a background effect. The Bowen blend was weak or absent. The ratio of the HeII line to the Hβ line decreased with time, indicating cooling.

5.3 V382 Vel

This is the oldest nova of our sample, observed twice, 13 and almost 14 yr respectively after the outburst, the longest time of all the classical novae in our sample. The emission lines of V382 Vel are markedly different from those of the other novae. The Bowen complex is very prominent, and all the lines are very broad, with a FWHM=1800 km s^{-1}. This emission may arise in material that has not slowed down significantly and is still expanding, but at this stage it is more likely that we are observing a spectrum originating in a wind from the accretion disc, and not the ejecta. There is an emission line complex close to the [O III] line at 5006 Å, already observed by others as early as 2011 (Tomov et al. 2015): it is due to two lines of Fe II at 4923 and 5018 Å and should not be confused with the nebular [O III].

5.4 HV Cet

In this nova the Bowen complex is practically absent, but the He II line at 4686 Å is still very strong, suggesting that there is still a hot ionizing source and that the plasma in which the He II originates is too dense for the Bowen blend. The [O III] lines are not detected after 6 yr.

5.5 U Sco

The SALT RSS spectra of U Sco are presented in the bottom panel of Fig. 11. The spectra do not differ from those measured by Tomov et al. (2015) in 2012 April, and they are remarkably similar to those observed at quiescence by Johnston & Kulkarni (1992) and by Dürbeck et al. (1993). The main characteristic of these spectra is that hydrogen lines in emission are almost absent. The only H line is the Hα, which is much weaker in the first spectrum and comparable with the He II line in the second. No other Balmer line was detected in emission, which indicates a remarkable hydrogen deficit in the accreted material. To our knowledge, because there are Balmer lines in emission in outburst, U Sco has never been modelled as a He nova, but the quiescent spectra are very intriguing in this respect.

Downloaded from https://academic.oup.com/mnras/article-abstract/480/4/4489/5078952
by Moscow State University, Scientific Library user
on 03 September 2018

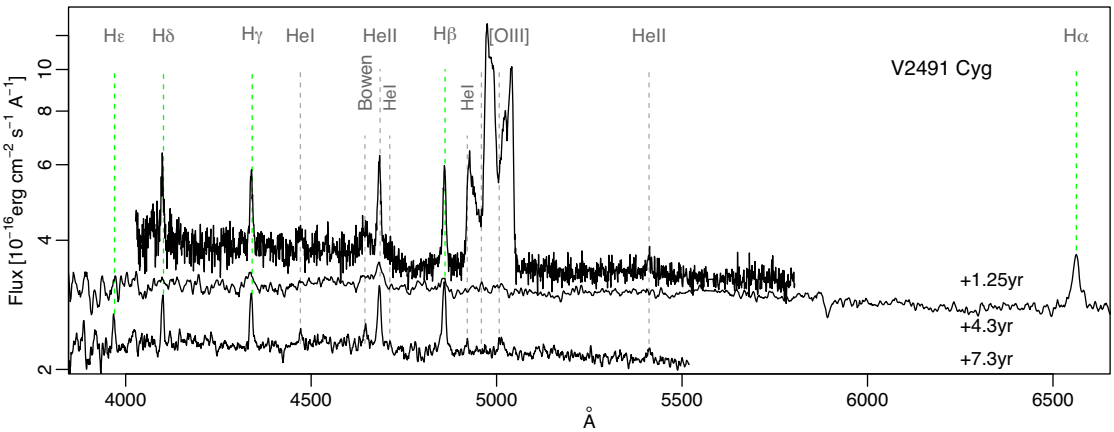

Figure 4. The evolution of the optical spectra of V2491 Cyg from outburst to quiescence. The time elapsed since the outburst is marked near each spectrum. The spectrum obtained 4.3 yr after the outburst is shifted upwards by 30 per cent for clarity.

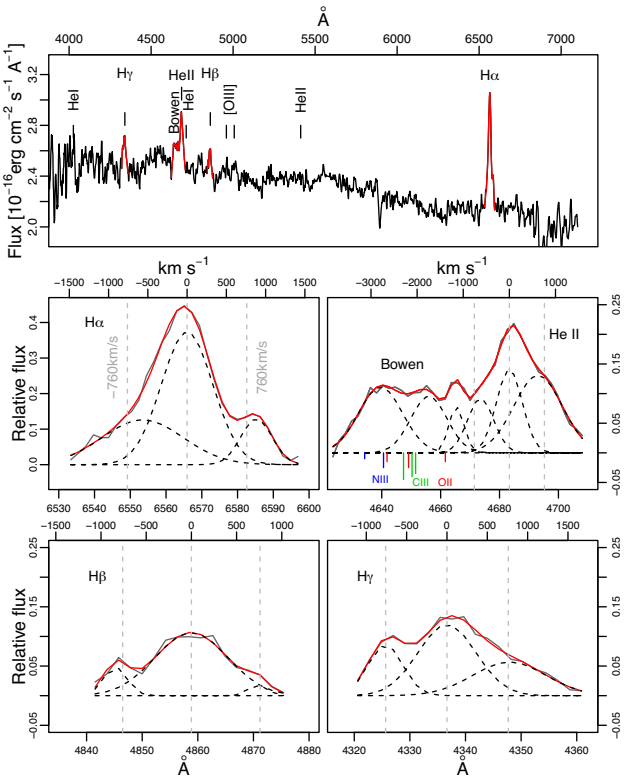

Figure 5. (Top) The flux-calibrated spectrum of V2491 Cyg, obtained in 2012. The strongest emission lines are marked. The result of the fit of the emission lines with a Gaussian component is plotted in red. (Bottom) The regions of the Balmer lines, the Bowen blend and the He II line after subtraction of the continuum. The red lines show the result of the fit, and the black-dashed lines show the Gaussian components that were introduced; for the main components of the Bowen blend we followed McClintock et al. (1975). The rest wavelength of the components of the fit for lines that constitute the Bowen blend is labelled.

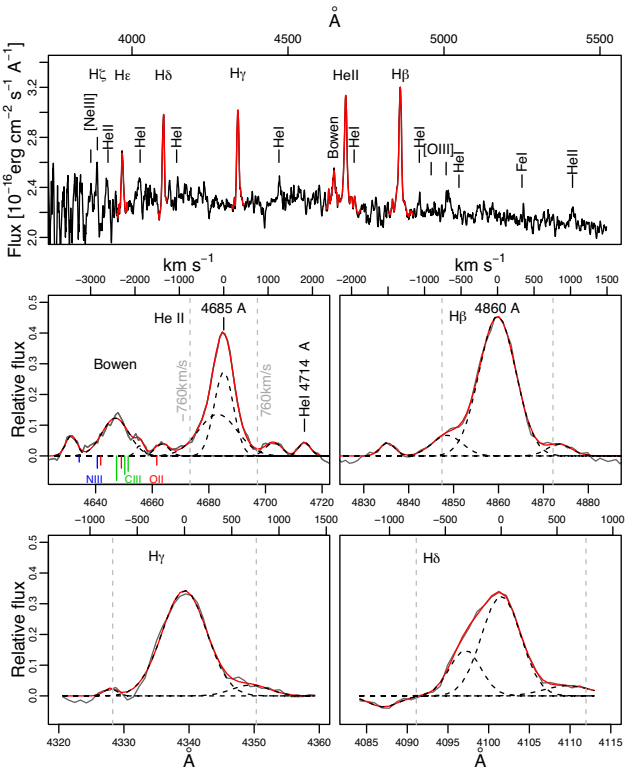

Figure 6. As Fig. 5, but for the observations of 2015.

5.6 Some general conclusions from this group of objects

Before proceeding to discuss the spectra of the symbiotic novae, we note that Fig. 9 shows a comparison of the quiescent spectra of five CNe: V4743 Sgr (published in Paper II), HV Cet, KT Eri, V2491 Cyg and V382 Vel. Measurements of EWs and fluxes are given in Table 4. Following Ringwald, Naylor & Mukai (1996) and Tomov et al. (2015), we plotted the EWs of the Hβ and HeII lines and the Bowen blend versus time elapsed after the explosion. The right panels of Fig. 10 show the trends in the novae of our sample. In the left panels we compare this group of mainly fast novae with the more general nova samples of Ringwald et al. (1996) and Tomov et al. (2015). The fast novae studied in this work tend to have higher ratios of EW(He II)/EW(Hβ), because, having been very luminous SSSs, they hosted hotter WDs from the beginning than the larger and more diverse group of objects studied by the above authors. However, we measured generally lower values of the emission-line EWs than in the larger and more diverse group of objects studied by the above authors. This may imply that the WD photosphere

Downloaded from https://academic.oup.com/mnras/article-abstract/480/4/4489/5078952
by Moscow State University, Scientific Library user
on 03 September 2018

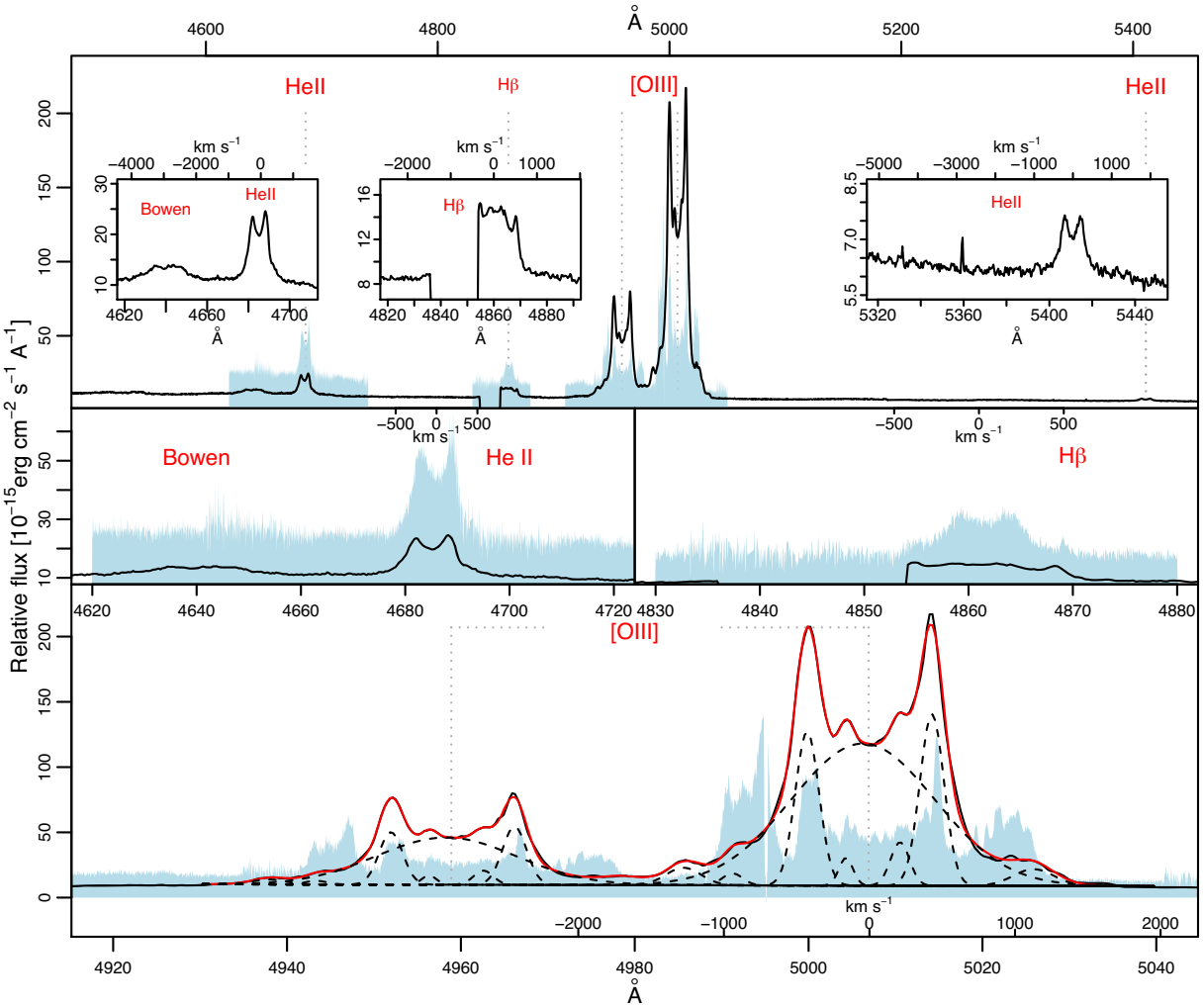

Figure 7. (Top) The spectrum of T Pyx. The insets show the regions of the He II and the Hβ lines. The blue shaded regions show the SALT spectrum of T Pyx obtained in 2014. (Bottom) The fit of the [O III] line of T Pyx with a number of Gaussians. The fit is shown with the red solid line, and the Gaussian components are plotted with the black dashed lines.

is cooling fast, reducing the number of photons with wavelengths shorter than the 228-Å edge, and consequently contributing less to the formation of the He II λ4686 line. We also note that in the repeated observations of KT Eri, V2491 Cyg and V382 Vel, the EWs of the emission lines decreased with time, with the exception of Hβ in the 2015 spectrum of V2491 Cyg, and the Bowen blend and the He II line in V382 Vel became weak within only 10 months, suggesting a fluctuating mass accretion rate in this nova.

6 THE SYMBIOTIC NOVAE

6.1 RS Oph

The SAAO spectra of RS Oph in two wavelength ranges, from 4000 to 4900 Å and from 6200 to 7000 Å, are presented in the top panel of Fig. 11. The dates of observations and the corresponding orbital phases are marked on the plot. The phases were calculated using the ephemerides presented in Brandi et al. (2009). The spectra show a pronounced variability of emission lines and the continuum.

We could reproduce the results of the previous authors, finding that the Balmer lines have broad pedestals, wings with FWHM ∼200–400 km s^{-1} and narrow, blue-shifted absorption features (FWHM∼70–80 km s^{-1}), as shown in Fig. 12. The pedestals have FWZI∼4000 km s^{-1}, which is larger than in previous observations by Brandi et al. (2009). While moderate changes of the central positions of the emission lines can be attributed to orbital motion, the pedestals of the Balmer lines and the shape of the continuum changed significantly between observations on time-scales as short as a day. It should be noted, however, that the fast and strong variability of the pedestals of the Balmer lines, which have a very asymmetric and irregular shape, affects the measurements of the central positions and the intensity of the narrow components. The double-peaked profile of the Balmer lines of RS Oph has been noted by several authors (see Section 2.8); however, the origin of the absorption components is still a matter of debate. Considering that absorption lines were still present 2 d after the nova explosion (Patat et al. 2011), Booth et al. (2016) concluded that they are produced in material at least 5×10^{13} cm away from the binary, which is probably an evaporative inflow to the poles that also produces the pedestals of the emission lines. The narrow component of the Balmer lines in our spectra is always red-shifted with respect to the absorption one, and the separation between them was ∼25 km

Downloaded from https://academic.oup.com/mnras/article-abstract/480/4/4489/5078952
by Moscow State University, Scientific Library user
on 03 September 2018

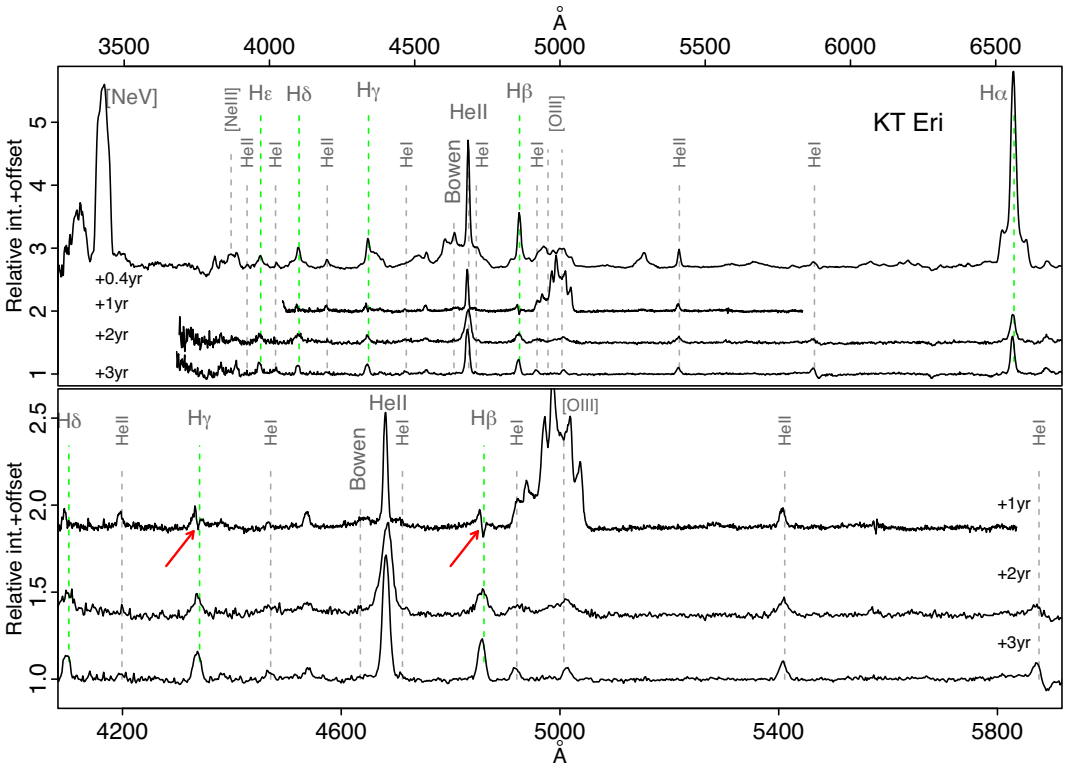

Figure 8. The evolution of the optical spectra of KT Eri from outburst to quiescence. The time elapsed since the outbursts is indicated. The bottom panel shows the quiescence spectra in more detail. The *y*-axis shows the relative intensity+arbitrary offset chosen for plotting purposes. Note the inverse P-Cyg profiles of the Balmer lines detected 1 yr after the explosion and marked on the plot with the red arrows.

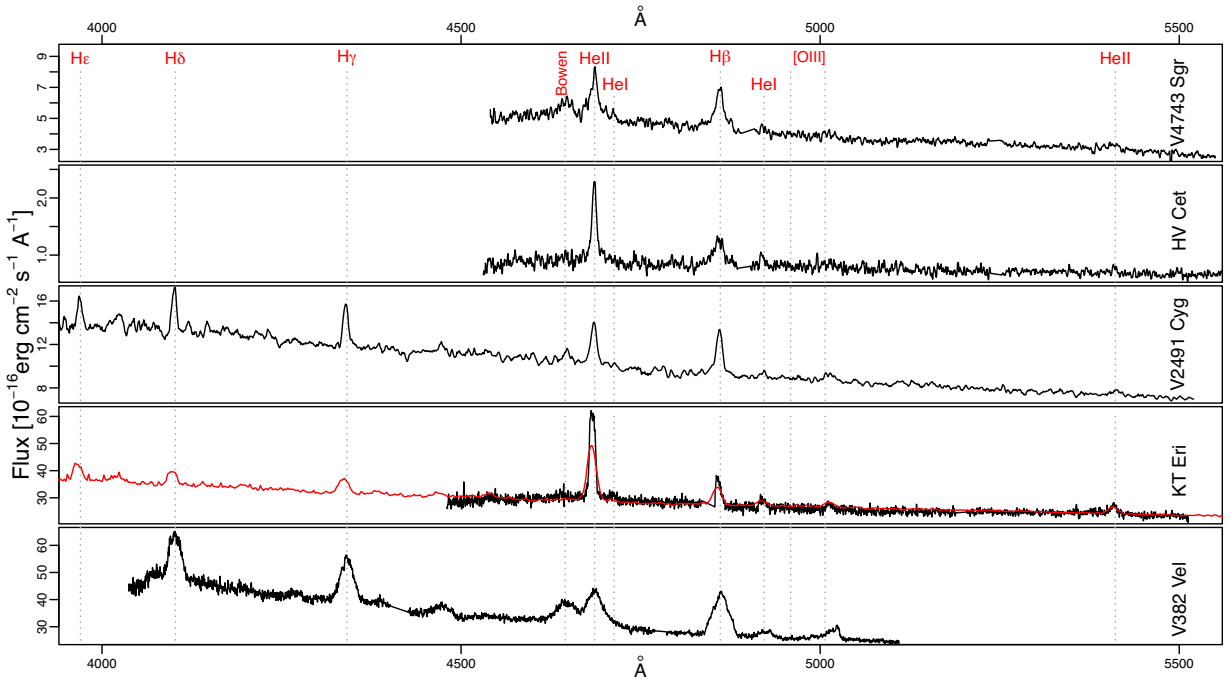

Figure 9. Spectra of V4743 Sgr, HV Cet, V2491 Cyg (only the last BTA spectrum), KT Eri (SALT in black, BTA in red) and V382 Vel (2013 spectrum). All the spectra were flux-calibrated and de-reddened except for the SALT spectrum of KT Eri, which we placed on the y-axis to match the continuum level of the other KT Eri spectrum obtained with the BTA, which has been flux-calibrated.

Downloaded from https://academic.oup.com/mnras/article-abstract/480/4/4489/5078952
by Moscow State University, Scientific Library user
on 03 September 2018

Table 4. Fluxes and equivalent widths of the emission lines of the sample novae, when measurable.

Nova	yr	Hα		Hβ		Hγ		Hδ		He II λ4686		Bowen blend	
		F^a	EW^b	F	EW	F	EW	F	EW	F	EW	F	EW
V4743 Sgr	3.3			63 ± 2	9.8 ± 0.1					74 ± 3	10.0 ± 0.2	36 ± 2	4.9 ± 0.2
	1.3			26.8 ± 0.4	7.8 ± 0.1	16.4 ± 0.3	4.7 ± 0.1	17.9 ± 0.3	5.2 ± 0.1	31.2 ± 0.7	8.7 ± 0.6	25 ± 2	6.9 ± 0.5
V2491 Cyg	4.3	26.2 ± 0.7	11.6 ± 0.2	4.7 ± 0.4	2.1 ± 0.1	7.0 ± 0.5	3.1 ± 0.1			12.0 ± 1.2	5.0 ± 0.5	10 ± 1	4.2 ± 0.5
	7.3			12.0 ± 0.2	5.5 ± 0.1	7.4 ± 0.2	3.3 ± 0.1	6.3 ± 0.1	2.8 ± 0.1	11.0 ± 0.2	5.0 ± 0.1	4.8 ± 0.2	2.2 ± 0.1
V382 Vel	13.9				15.4 ± 0.1		10.4 ± 0.1		7.9 ± 0.1		12.4 ± 0.5		7.3 ± 0.5
	1										19.1 ± 0.1		1.5 ± 0.1
KT Eri	2		10.4 ± 0.1		4.2 ± 0.1		2.4 ± 0.4		4.2 ± 0.5		14 ± 0.3		1 ± 0.3
	3	151 ± 1	10.3 ± 0.1	75 ± 1	3.5 ± 0.1	60 ± 10	2.6 ± 0.4	55 ± 10	2.2 ± 0.4	247 ± 3	11.3 ± 0.2	13 ± 12	0.6 ± 0.1
	3									244 ± 3	12.7 ± 0.1		
HV Cet	3.3			4.9 ± 0.4	9.7 ± 0.3					7.6 ± 0.3	14 ± 0.5		

[a]Flux ($\times 10^{-16}$ erg cm^{-2} s^{-1}), [b]equivalent width (Å)

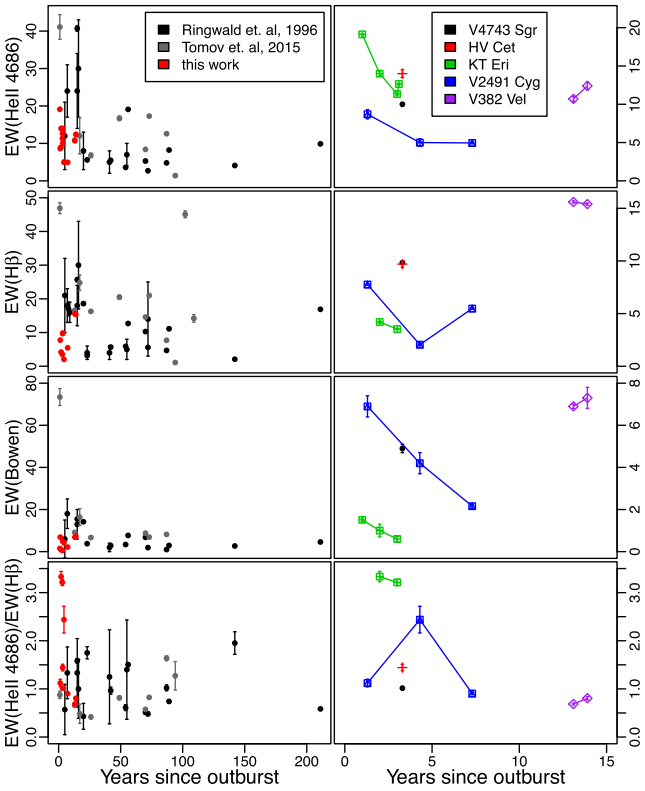

Figure 10. Equivalent widths of the He II, Hβ and the Bowen blend versus time. The panels on the left show our data (red) in comparison with those of Ringwald et al. (1996) (black) and of Tomov et al. (2015) (grey). The right panel shows only the data obtained in this work.

s^{-1} in the observations performed in 2011 and only ∼10 km s^{-1} in 2012, so we confirm that its motion does not correlate with either the WD or the red giant, as inferred by Brandi et al. (2009).

The spectra also show numerous emission lines of Fe I and Fe II and the absorption lines of Ti I, the latter originating in the giant secondary. The He II line and the Bowen blend are weak, and their intensity changed between 2011 and 2012, probably because they were observed at different orbital phases. All our spectra show the unambiguous presence of the Li I doublet, with a clear absorption features at λ6708, discovered before us by Brandi et al. (2009). However, these authors found that it originates in the secondary, and cannot be used to investigate lithium nucleosynthesis in the thermonuclear runaway.

6.2 V3890 Sgr

Six spectra of V3890 Sgr are shown in the middle panel of Fig. 11 and in Fig. 13. They reveal an Hα line structure similar to that of RS Oph: emission with broad wings and a central absorption feature (see Fig. 13). The FWHM of the Hα line lies in the range 95–105 km s^{-1}, the broad component has FWHM ∼ 300 km s^{-1}, and the absorption component 60–80 km s^{-1}. The moderate changes of the intensity and central position of the Hα line components probably reflect the orbital motion. The spectra show the Balmer lines and lines of He I, [O I], and very weak He II at 4686 Å.

Downloaded from https://academic.oup.com/mnras/article-abstract/480/4/4489/5078952
by Moscow State University, Scientific Library user
on 03 September 2018

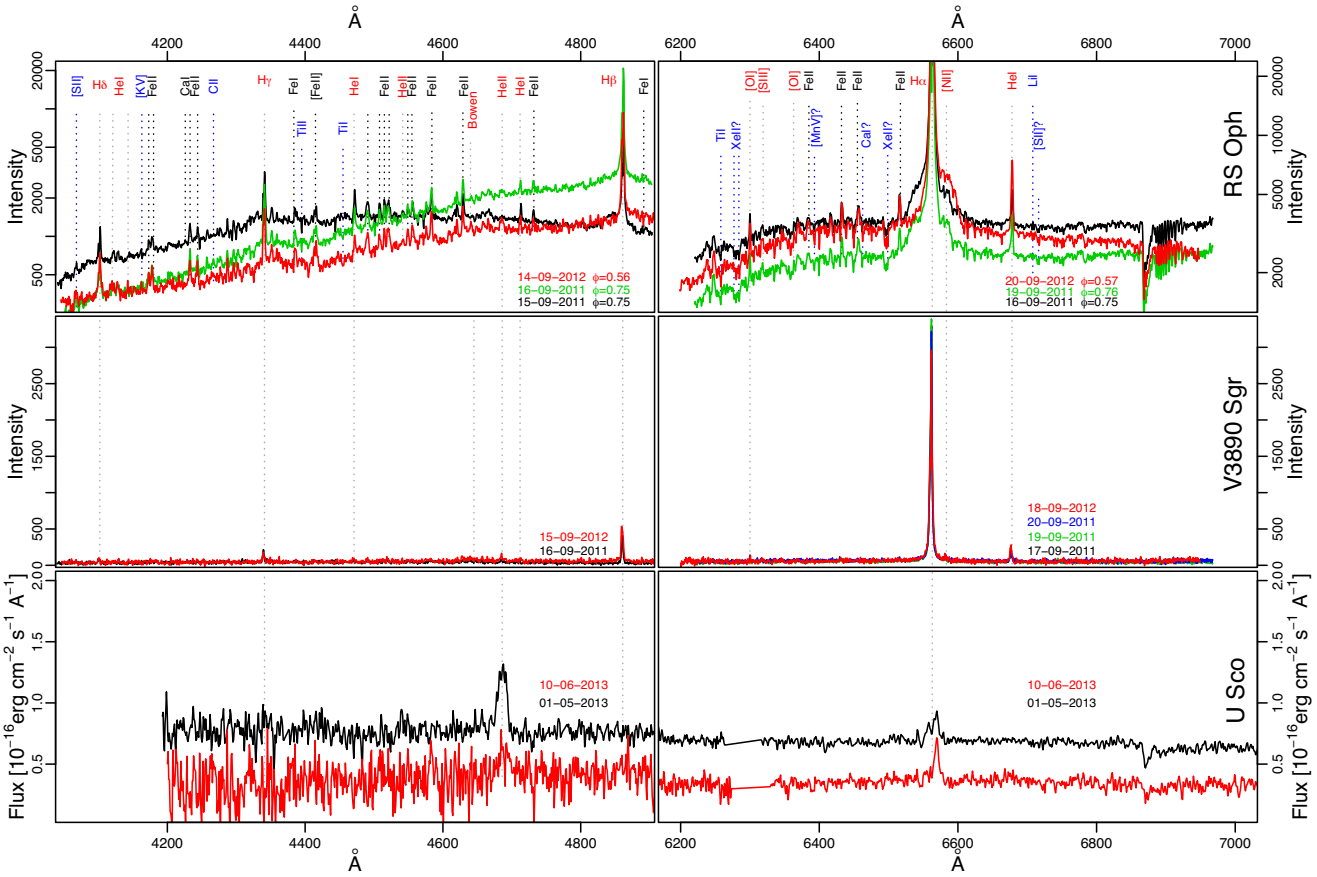

Figure 11. The SAAO spectra of RS Oph and V382 Vel and the SALT spectra of U Sco. The dates of the observations are marked in each panel. For RS Oph we also indicate the orbital phase.

7 CONCLUSIONS

(i) **Novae as IP candidates.** The optical photometry we have presented, in which we clearly detect the beat period of the rotation and spin periods for V4743 Sgr and a periodicity that may be attributed to the beat period also for V2491 Cyg, confirms the classification of the first nova as an IP and gives some credibility to the suggestion that this second nova is also an IP. Moreover, the optical spectra of V2491 Cyg do not show double-peaked profiles, possibly indicating a low inclination and explaining why the orbital period has never been detected. These optical spectra also present another possible diagnostic of an IP, namely a second component in the emission lines. In fact, the measurement of the beat period in the optical offers a method to investigate the magnetic nature of cataclysmic variables, although detection of the spin period in X-rays has so far been considered the best indirect proof of an IP. The shrinking region that still emits supersoft X-ray flux in V4743 Sgr and V2491 Cyg is also likely to be connected to a delayed quenching of the nuclear burning at the poles, or to an inhomogeneous atmosphere on the WD, two interpretations that have been proposed for recent observations of V407 Lup, another nova that is also an IP (Aydi et al. 2018).

(ii) **How the 'weird' T Pyx is different.** Ringwald et al. (1996) found that the rate of fading of nebular lines is dependent only on the speed class of the nova. Theoretical models predict that slow novae eject larger envelopes. We expect that the time for the nebular lines to disappear is an indication of the time required to disperse the ejecta in the interstellar medium. This should be a function of both the ejection velocity and the mass of the ejecta, which are anti-correlated in the simulations. Therefore, for slow novae we expect that the [O III] lines will last for much longer periods than for fast novae, which tend to have higher ejection velocities and smaller ejecta masses. Indeed, we find that T Pyx maintains much more prominent [O III] lines than the other, faster novae we observed spectroscopically.

Most interestingly, the high-resolution optical spectra of T Pyx show a fragmented and complicated structure in the [O III] nebular lines, supporting a scenario in which the shell fragmentation is caused by the outflow mode and not by later instabilities occurring in the shell.

(iii) **How long, and why, do the nova WDs remain hot?** The spectra of five CNe, presented in Fig. 9, are very similar, but V382 Vel has much broader lines than the other novae. These spectra show prominent He II lines, and the Bowen blend is also still present in all, except in KT Eri. We note that Williams & Ferguson (1983) stress that 'The fluorescence mechanism requires: 1) high line resonance optical depths to produce trapping of the line radiation so conversion to optical transitions can take place, 2) densities which are sufficiently low such that collisional de-excitation of the levels does not occur, 3) relatively small velocity gradients within the emitting volume to ensure the "tuning" between the [O III] and the N III resonant transitions.'

It follows that the conditions for the λ4686 He II and for the Bowen blend may be quite different, but both can originate in inner zones of the accretion disc and their relative strength with respect to Hβ is an indication of high $\dot{m}$. However, because the Bowen blend

Downloaded from https://academic.oup.com/mnras/article-abstract/480/4/4489/5078952
by Moscow State University, Scientific Library user
on 03 September 2018

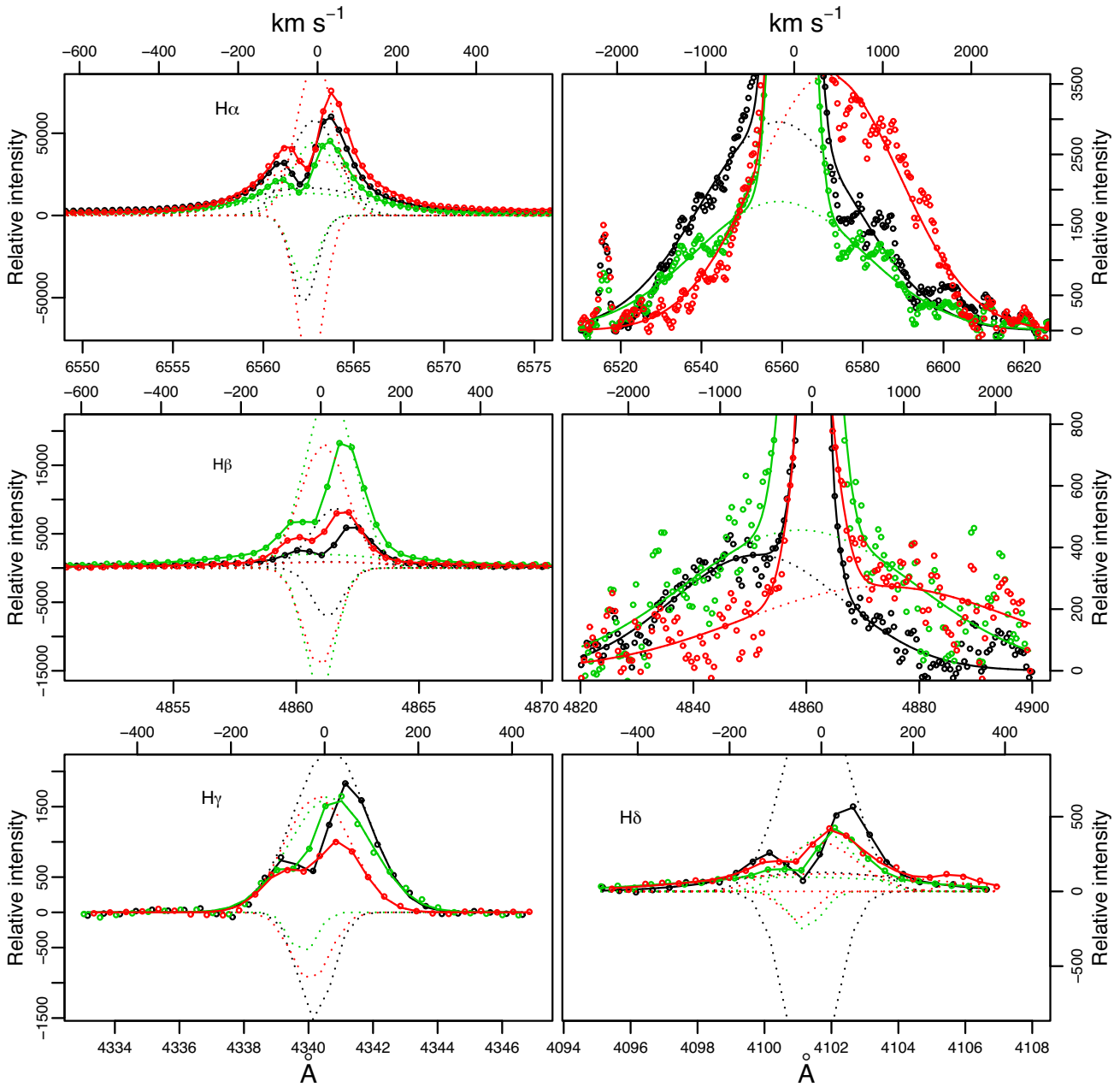

Figure 12. The fits to the emission lines of RS Oph. The different epochs are colour-coded as in the top panel of Fig. 11. The left panels show the double-peaked emission lines and how we modelled them with one or two Gaussians for the broad emission, and one narrow Gaussian for the blue-shifted absorption. The top two panels on the right show the broad pedestals of the two main Balmer lines. The solid lines show the results of the fits with a number of Gaussian components, while the dashed lines show the single Gaussian components used in the fit. .

requires low density, the He II line may also originate in a medium with density that is too high for the Bowen blend. The Bowen blend may have its origin in the decelerated, ejected nova shell, while the HeII line at this post-outburst stage is always formed in the accretion disc or accretion stream. In any case, both the ratio of the Bowen blend to Hβ and that of the HeII line to Hβ can trace the cooling of the WD atmosphere as it returns to quiescence; large ratios should indicate that mass transfer has resumed at a high rate because of irradiation of the secondary.

However, after comparing our measurements with those of Ringwald et al. (1996) and Tomov et al. (2015), we found that the equivalent widths of the Hβ, He II and Bowen blend and the ratios, of the intensity and especially of the EW, of HeII and the Bowen blend to that of Hβ do not seem to be correlated with post-outburst age. Neither do we find a correlation with orbital period, as would be expected if irradiation triggers mass transfer, confirming the results by Ringwald et al. (1996) and Tomov et al. (2015).

There has been speculation in the literature that short-period systems have longer SSS phases because the burning is refuelled by the enhanced mass accretion of an irradiated secondary (e.g. Greiner, Orio & Schartel 2003). Enhanced mass transfer in the early post-outburst phase, dependent on the orbital separation, is also predicted in the hibernation scenario (Shara et al. 1986; Kovetz, Prialnik & Shara 1988): a period of high $\dot{m}$ would precede and follow

Downloaded from https://academic.oup.com/mnras/article-abstract/480/4/4489/5078952
by Moscow State University, Scientific Library user
on 03 September 2018

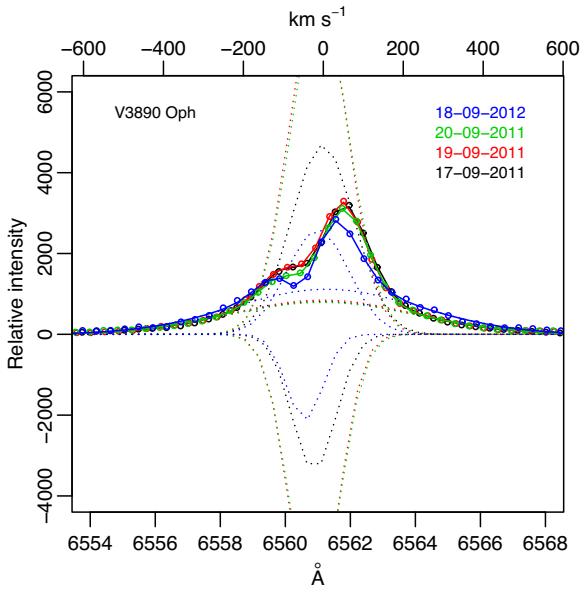

Figure 13. As Fig. 12, for the Hα line of V3890 Sgr.

every nova explosion, with a long inter-outburst period at very low $\dot{m}$ in between. After observational evidence discovered by Naylor et al. (1992) against the hibernation scenario, Ringwald et al. (1996), and more recently Tomov et al. (2015), found that the intensity ratio of the He II and Bowen lines to Hβ does not appear to become weaker in very old novae, indicating a steady average $\dot{m}$ on long time-scales. However, Ringwald et al. (1996) also discovered that several very old novae cannot be spectroscopically identified, a fact that may imply that they have stopped (or almost stopped) accreting. If hibernation occurs, we expect the ratio of the He II and Bowen lines to Hβ to be large and to remain so, because of the high mass transfer rate triggered after the outburst, with inverse dependence on the orbital period, because a short orbital distance allows more effective irradiation. Our data support, albeit marginally, the lack of evolution of the lines' EW ratios, but we did not find any clear correlation with the orbital periods given in Table 1.

(iv) The symbiotic novae. Finally, we must note the difference between the spectra of RS Oph and V3890 Sgr and of most symbiotics that are 'permanent' SSSs and appear to be burning hydrogen steadily (see e.g. the spectrum of SMC 3 in Orio et al. 2007). There is a symbiotic in M31 that does not have coronal lines of [Fe X] and seems to be a steady nuclear burner, but it is a steady SSS source (Orio et al. 2017). In that system, the plasma density must be higher than 5×10^9 cm^{-3} to avoid the formation of coronal lines, but the inclination of the disc and the filling factor of the nebular material must be such to allow the SSS to be observed directly. However, RS Oph and V3890 Sgr are not persistent SSSs, and they do not emit coronal lines. Furthermore, the absence or extreme weakness of He II at 4686 Å in RS Oph and V3890 Sgr indicates either that the WD has completely cooled or that there is very high-density material in the binary. Hydrogen-burning is intermittent in the RN-symbiotics. We would like to suggest a possible interpretation of this phenomenon: most likely, it is because the mass transfer rate itself is intermittent and pauses between outbursts, or in any case it does not occur at a constant rate.

ACKNOWLEDGEMENTS

We thank N.V. Metlova for her observations of HV Cet that we presented in the paper. This paper is based on observations made at the South African Astronomical Observatory (SAAO, A. PI Odendaal) and at the South African Large Telescope (SALT, PI M. Orio), obtained under programs 830-4 2012-2-UW-004, 1096-5 2013-1-UW_OTH-001, 1275-6 2013-2-UW-006, 1178-7 2013-2-UW-001, 1178-7 2013-2-UW-001. EB was funded by the Russian Foundation for Basic Research, research project no. 16-02-00758. AFV is supported by the Russian Science Foundation under grant 14-50-00043. The CSS survey is funded by the National Aeronautics and Space Administration under grant no. NNG05GF22G issued through the US Science Mission Directorate Near-Earth Objects Observations Program. The CRTS survey is supported by the US National Science Foundation under grants AST-0909182 and AST-1313422. The work on V2491 Cyg and V4743 Sgr reported in this paper is included in PZ's PhD thesis, funded by the CARIPARO Foundation at the University of Padova.

REFERENCES

Adamakis S., Eyres S. P. S., Sarkar A., Walsh R. W., 2011, MNRAS, 414, 2195
Augusto A., Diaz M. P., 2003, AJ, 125, 3349
Aydi E. et al., 2018, MNRAS, 480, 582
Baklanov A., Pavlenko E., Berezina E., 2008, Astron. Telegram, 1514, 1
Balman Ş., Retter A., Bos M., 2006, AJ, 131, 2628
Barry R. K., Mukai K., Sokoloski J. L., Danchi W. C., Hachisu I., Evans A., Gehrz R., Mikolajewska J., 2008, in Evans A., Bode M. F., O'Brien T. J., Darnley M. J., eds, Astronomical Society of the Pacific Conference Series Vol. 401, RS Ophiuchi (2006) and the Recurrent Nova Phenomenon. Astron. Soc. Pac., San Francisco, p. 52
Beardmore A. P. et al., 2012, A&A, 545, A116
Bianchini A., Canterna R., Desidera S., Garcia C., 2003, PASP, 115, 474
Bode M. F. et al., 2006, ApJ, 652, 629
Booth R. A., Mohamed S., Podsiadlowski P., 2016, MNRAS, 457, 822
Bos M., Retter A., McCormick J., Velthuis F., 2001, IAU Circ., 7610
Bowen I. S., 1934, PASP, 46, 146
Bowen I. S., 1935, ApJ, 81, 1
Brandi E., Quiroga C., Mikołajewska J., Ferrer O. E., García L. G., 2009, A&A, 497, 815
Burstein D., Heiles C., 1982, AJ, 87, 1165
Cardelli J. A., Clayton G. C., Mathis J. S., 1989, in Allamandola L. J., Tielens A. G. G. M., eds, Proc. IAU Symp. 135, Interstellar Dust. Kluwer, Dordrecht, p. 5
Chesneau O. et al., 2007, A&A, 464, 119
Darnley M. J., Ribeiro V. A. R. M., Bode M. F., Munari U., 2011, A&A, 530, A70
Deeming T. J., 1975, Ap&SS, 36, 137
Della Valle M., Pasquini L., Daou D., Williams R. E., 2002, A&A, 390, 155
Dobrotka A., Ness J.-U., 2010, MNRAS, 405, 2668
Drake A. J. et al., 2009a, ApJ, 696, 870
Drake A. J. et al., 2009b, Astron. Telegram, 1940
Drake A. J. et al., 2009c, Astron. Telegram, 2331
Duerbeck H. W., 1987, Space Sci. Rev., 45, 1
Dürbeck H. W., Dümmler R., Seitter W. C., Leibowitz E. M., Shara M. M., 1993, Messenger, 71, 19
Eyres S. P. S. et al., 2009, MNRAS, 395, 1533
Ferrario L., 1991, in Bertout C., Collin-Souffrin S., Lasota J. P., eds, Poc. IAU Colloq. 129, The 6th Institute d'Astrophysique de Paris (IAP) Meeting: Structure and Emission Properties of Accretion Disks. Kluwer, Dordrecht, p. 425
Gilmore A. C., Kilmartin P. M., 1999, IAU Circ., 7238
Gilmozzi R., Selvelli P., 2007, A&A, 461, 593
González-Riestra R., 2015, Acta Polytechnica CTU Proc., 2, 252

Downloaded from https://academic.oup.com/mnras/article-abstract/480/4/4489/5078952
by Moscow State University, Scientific Library user
on 03 September 2018

Goranskij V. P., Metlova N. V., 2009, Astron. Telegram, 1938
Greiner J., Orio M., Schartel N., 2003, A&A, 405, 703
Hachisu I., Kato M., 2009, ApJ, 694, L103
Hachisu I., Kato M., Kato T., Matsumoto K., Nomoto K., 2000, ApJ, 534, L189
Haseda K., West D., Yamaoka H., Masi G., 2002, IAU Circ., 7975, 1
Hounsell R. et al., 2010a, ApJ, 724, 480
Hounsell R. et al., 2010b, Astron. Telegram, 2558
Ibarra A. et al., 2009, A&A, 497, L5
Iijima T., 2009, A&A, 505, 287
Imamura K., Tanabe K., 2012, PASJ, 64
Itagaki K., 2009, Cent. Bur. Elect. Teleg., 2050
Johnston H. M., Kulkarni S. R., 1992, ApJ, 396, 267
Jurdana-Sepic R., Munari U., 2008, Inf. Bull. Variable Stars, 5839, 1
Jurdana-Šepić R., Ribeiro V. A. R. M., Darnley M. J., Munari U., Bode M. F., 2012, A&A, 537, A34
Kang T. W., Retter A., Liu A., Richards M., 2006, AJ, 132, 608
Kastner S. O., Bhatia A. K., 1996, MNRAS, 279, 1137
Kilmartin P., Gilmore A., Jones A. F., Pearce A., 1990, IAU Circ., 5002
Kovetz A., Prialnik D., Shara M. M., 1988, ApJ, 325, 828
Krautter J., 2008, in Evans A., Bode M. F., O'Brien T. J., Darnley M. J., eds, Astronomical Society of the Pacific Conference Series Vol. 401, RS Ophiuchi (2006) and the Recurrent Nova Phenomenon. Astron. Soc. Pac., San Francisco, p. 139
Landolt A. U., 1992, AJ, 104, 340
Leibowitz E., Orio M., Gonzalez-Riestra R., Lipkin Y., Ness J.-U., Starrfield S., Still M., Tepedelenlioglu E., 2006, MNRAS, 371, 424
McClintock J. E., Canizares C. R., Tarter C. B., 1975, ApJ, 198, 641
Mikołajewska J., Shara M. M., 2017, ApJ, 847, 99
Morales-Rueda L., Still M. D., Roche P., 1999, MNRAS, 306, 753
Munari U., Siviero A., Dallaporta S., Cherini G., Valisa P., Tomasella L., 2011, New A *stron.*, 16, 209
Nakano S. et al., 2008, IAU Circ., 8934, 1
Naylor T., Charles P. A., Mukai K., Evans A., 1992, MNRAS, 258, 449
Nelson T., Orio M., Cassinelli J. P., Still M., Leibowitz E., Mucciarelli P., 2008, ApJ, 673, 1067
Ness J.-U. et al., 2003, ApJ, 594, L127
Ness J.-U., Starrfield S., Jordan C., Krautter J., Schmitt J. H. M. M., 2005, MNRAS, 364, 1015
Ness J.-U. et al., 2007, ApJ, 665, 1334
Ness J.-U. et al., 2009, AJ, 137, 3414
Ness J.-U. et al., 2011, ApJ, 733, 70
Ness J.-U. et al., 2012, ApJ, 745, 43
Ness J.-U. et al., 2014, Astron. Telegram, 6147
Nielbock M., Schmidtobreick L., 2003, A&A, 400, L5
O'Brien T. J. et al., 2006, Nature, 442, 279
Orio M., 2012, Bull. Astron. Soc. India, 40, 333
Orio M., Covington J., Ögelman H., 2001a, A&A, 373, 542
Orio M., Covington J., Ögelman H., 2001b, A&A, 373, 542
Orio M., Zezas A., Munari U., Siviero A., Tepedelenlioglu E., 2007, ApJ, 661, 1105
Orio M. et al., 2013, MNRAS, 429, 1342
Orio M. et al., 2017, MNRAS, 470, 2212
Page K. L. et al., 2010, MNRAS, 401, 121
Pagnotta A. et al., 2015, ApJ, 811, 32
Patat F., Chugai N. N., Podsiadlowski P., Mason E., Melo C., Pasquini L., 2011, A&A, 530, A63
Patterson J. et al., 1998, PASP, 110, 380
Patterson J. et al., 2014, in Woudt P. A., Ribeiro V. A. R. M., eds, Astronomical Society of the Pacific Conference Series Vol. 490, Stellar Novae: Past and Future Decades. Astron. Soc. Pac., San Francisco, p. 35
Pavlenko Y. V. et al., 2016, MNRAS, 456, 181
Pejcha O., Prieto J. L., Denney K., 2008, Astron. Telegram, 1825
Prieto J. L., Denney K., Pejcha O., Wagner R. M., 2008, Astron. Telegram, 1835
Ragan E. et al., 2009, Astron. Telegram, 2327
Rauch T., Orio M., Gonzales-Riestra R., Nelson T., Still M., Werner K., Wilms J., 2010, ApJ, 717, 363
Ribeiro V. A. R. M. et al., 2009, ApJ, 703, 1955
Ribeiro V. A. R. M., Darnley M. J., Bode M. F., Munari U., Harman D. J., Steele I. A., Meaburn J., 2011, MNRAS, 412, 1701
Richards M. T., Kang T. W., Retter A., Liu A., 2005, in Am. Astron. Soc. Meeting Abstracts. 207.7020
Ringwald F. A., Naylor T., Mukai K., 1996, MNRAS, 281, 192
Rudy R. J., Lynch D. K., Russell R. W., Woodward C. E., Covey K., 2008, IAU Circ., 8938, 2
Scargle J. D., 1982, ApJ, 263, 835
Schaefer B. E., 1990, ApJ, 355, L39
Schaefer B. E., 2010, ApJS, 187, 275
Schaefer B. E. et al., 2010, AJ, 140, 925
Schaefer B. E. et al., 2013, ApJ, 773, 55
Schwarz G. J. et al., 2008, Astron. Telegram, 1847
Schwarz G. J. et al., 2011, ApJS, 197, 31
Selvelli P., Cassatella A., Gilmozzi R., González-Riestra R., 2008, A&A, 492, 787
Shara M. M., Livio M., Moffat A. F. J., Orio M., 1986, ApJ, 311, 163
Shara M. M., Zurek D. R., Williams R. E., Prialnik D., Gilmozzi R., Moffat A. F. J., 1997, AJ, 114, 258
Shore S. N. et al., 2003, AJ, 125, 1507
Shugarov S. Y., Chochol D., Volkov I. M., Zemko P. O., 2010, in Sterken C., Samus N., Szabados L., eds, Variable Stars, The Galactic halo and Galaxy Formation. Sternberg Astronomical Institute of Moscow University, Russia, Moscow, p. 198
Sokoloski J. L., Rupen M. P., Mioduszewski A. J., 2008, ApJ, 685, L137
Strope R. J., Schaefer B. E., Henden A. A., 2010, AJ, 140, 34
Surina F., Hounsell R. A., Bode M. F., Darnley M. J., Harman D. J., Walter F. M., 2014, AJ, 147, 107
Takei D., Ness J.-U., Tsujimoto M., Kitamoto S., Drake J. J., Osborne J. P., Takahashi H., Kinugasa K., 2011, PASJ, 63, 729
Thoroughgood T. D., Dhillon V. S., Littlefair S. P., Marsh T. R., Smith D. A., 2001, MNRAS, 327, 1323
Tofflemire B. M., Orio M., Page K. L., Osborne J. P., Ciroi S., Cracco V., Di Mille F., Maxwell M., 2013, ApJ, 779, 22
Tomov T., Swierczynski E., Mikolajewski M., Ilkiewicz K., 2015, A&A, 576, A119
Toraskar J., Mac Low M.-M., Shara M. M., Zurek D. R., 2013, ApJ, 768, 48
Vanderburg A., Johnson J. A., 2014, PASP, 126, 948
Vanlandingham K. M., Schwarz G., Starrfield S., Woodward C., Wagner M., Ness J., Helton A., 2007, in Am. Astron. Soc. Meeting Abstracts, 210, 99
Vaytet N. M. H., O'Brien T. J., Page K. L., Bode M. F., Lloyd M., Beardmore A. P., 2011, ApJ, 740, 5
Wagner R. M., Steinfadt J., Bond H. E., Hooper E., Karam A., Rohrbach J., Schwarz G., Starrfield S., 2005, in Am. Astron. Soc. Meeting Abstracts, 207.7023
Williams R. E., Ferguson D. H., 1983, in Livio M., Shaviv G., eds, Astrophysics and Space Science Library Vol. 101, IAU Colloq. 72, Cataclysmic Variables and Related Objects. Kluwer, Dordrecht, p. 97
Williams P., Lee S., Pearce A., Gilmore A. C., Pollard K. R., McSaveney J. A., Kilmartin P. M., Caldwell P., 1999, IAU Circ., 7176
Wolf W. M., Bildsten L., Brooks J., Paxton B., 2013, ApJ, 777, 136
Woodward C. E., Wooden D. H., Pina R. K., Fisher R. S., 1999, IAU Circ., 7220
Worters H. L., Rushton M. T., 2014, MNRAS, 442, 2637
Zamanov R. K., 2011, Bulg. Astron. J., 17, 59
Zemko P., Mukai K., Orio M., 2015, ApJ, 807, 61
Zemko P., Orio M., Mukai K., Bianchini A., Ciroi S., Cracco V., 2016, MNRAS, 460, 2744

This paper has been typeset from a TEX/LATEX file prepared by the author.

Downloaded from https://academic.oup.com/mnras/article-abstract/480/4/4489/5078952
by Moscow State University, Scientific Library user
on 03 September 2018